한국기계가공학회지, 제20권, 제5호, pp. 76～84(2021.05) ISSN 1598-6721(Print)
Journal of the Korean Society of Manufacturing Process Engineers, Vol. 20, No. 5, pp. 76~84(2021.05) ISSN 2288-0771(Online)

https://doi.org/10.14775/ksmpe.2021.20.05.076

Optimal Stiffness Design of Self-Piercing Riveting's C-Frame for Multimaterial Joining

Chang-Yeul Shin*, Jae-Jin Lee*, Ji-Hun Mun*, Soon-Deok Kwon*,
Min-Seok Yang**, Jae-Wook Lee**,#

*Gyeong-Buk Hybrid Technology Institute, **Korea Institute of Industrial Technology

다종소재 접합을 위한 SPR(Self-Piercing Riveting)용 C-프레임 강성 최적설계

신창열*, 이재진*, 문지훈*, 권순덕*, 양민석**, 이재욱**,#

*경북하이브리드부품연구원, **한국생산기술연구원

(Received 17 March 2021; received in revised form 01 April 2021; accepted 03 April 2021)

ABSTRACT

In this study, an optimal stiffness model of the C-frame, which was supporting the mold and tool load, was proposed to obtain quality self-piercing riveting (SPR) joining. First, the load path acting on the C-frame structure was identified using topology optimization. Then, a final suggested model was proposed based on the load path results. Stiffness and strength analyses were performed for a rivet pressing force of 7.3 [t] to compare the design performance of the final proposed model with that of the initial model. Moreover, to examine the reliability of continuous and repeated processes, vibration analysis was performed and the dynamic stiffness of the final proposed model was reviewed. Additionally, fatigue analysis was performed to ascertain the fatigue characteristics due to simple repetitive loading. Finally, stiffness test was performed for the final proposed model to verify the analysis results. The obtained results differed from the analysis result by 2.9%. Consequently, the performance of the final proposed model was superior to that of the initial model with respect to not only the SPR fastening quality but also the reliability of continuous and repetitive processes.

Key Words : Multi-Material Joining(다종재료 결합), Self-Piercing Riveting(셀프 피어싱 리벳), C-Frame(C 프레임), Topology Optimization(위상 최적화), Stiffness Optimization(강성 최적화)

1. INTRODUCTION

In response to tightening environmental and fuel economy regulations, the manufacturers of complete vehicles have recently been increasingly conducting research to lightweight the car body, increase the efficiency of the engine and drivetrain, and reduce running resistance. Reduction in curb weight by 5% can improve fuel economy and power performance by 1.5% and 4.5%, respectively. Additionally, improvement in

Corresponding Author : jaewk@kitech.re.kr
Tel: +82-53-580-0186, Fax: +82-53-580-0130

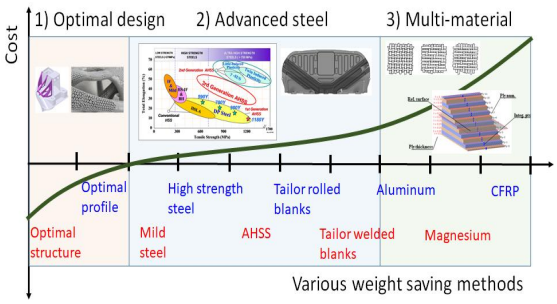

Fig. 1 Various light-weight technology for BIW[1,2]

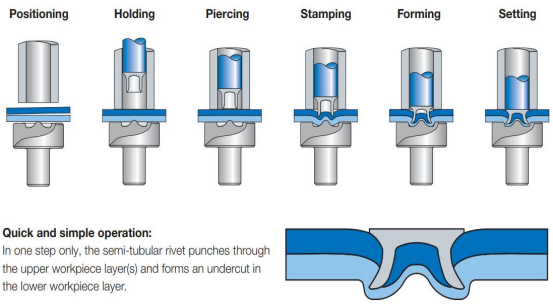

Fig. 2 SPR joinning process for multi-material plates[3]

Fig. 3 C-Frame for SPR joinning process[3]

collision performance by 4.5% and reducing inertial load can improve the durability of autobody parts. Therefore, the application of multi-materials, such as advanced high strength steel, aluminum, magnesium, and carbon fiber reinforced plastics (CFRP), is growing (Fig. 1).[1,2]

The task of joining the parts with disparate mechanical properties has arisen with the increase in multi-materials usage. Welding is the conventional joining technology for a car body; Additionally, laser welding, point welding, and arc welding have also been widely used. However, welding methods involve welding gas release; therefore, it may be difficult to meet the environmental regulatory standards. It is a challenge to use welding technology to join the multi-materials, each having different mechanical properties. There may be quality defects due to thermal distortion. Additionally, the use of non-ferrous materials, such as polymer, has increased, where the traditional welding methods are not involved.

Furthermore, mechanical joining using bolts, nuts, and rivets is disadvantageous because it requires creating holes, adding an extra manufacturing process. Moreover, automatizing the manufacturing process is a challenge due to possible problems associated with misalignment between holes and bolts. Additionally, joining requires post-processing, increasing the total processing time.

Self-piercing rivet (SPR) is the commonly used joining method for multi-materials, such as aluminum. It is a mechanical method, which does not require stopping the manufacturing. In this method, a tooth-shaped rivet is pressed by force using a puncture inside the top holder after joining the multi-materials, as shown in Fig. 2.[2,4-6] Rivet can be fastened by press-fit molding; hence, thermal distortion does not occur between the materials with different mechanical properties. Rivet fastening can replace point welding, the traditional molding-based method—the rivet penetrates the top plate, and then its leg conforms to the shape of the mold beneath the bottom plate to join the target materials. SPR does not require separate hole manufacturing. Its automation is possible because its processing time is short, and the process does not create a useless byproduct. Its shape is the same as the

C-frame of point welding equipment, replacing the traditional facility. Moreover, SPR has high fatigue properties and a similar fastening strength as point welding. However, the stiffness of the C-frame determines the fastening quality due to press-fit force because C-frame supports the fit force of a rivet (see Fig. 4). Furthermore, the joint should be robust against the vibrational load in continuous operation, and the fatigue properties of the press-fit force should be tested. Specifically, it requires stiffness design optimization due to these differences.[7-8] This study focuses on conducting a topology design optimization of the C-frame supporting the loads of the mold and tools to obtain SPR fastening quality. Additionally, we performed the C-frame design optimization for the stiffness and strength due to the press-fit force. Furthermore, we intend to establish the reliability of the C-frame design for continuous repetitive manufacturing via vibrational and fatigue analysis of the proposed C-frame structure.

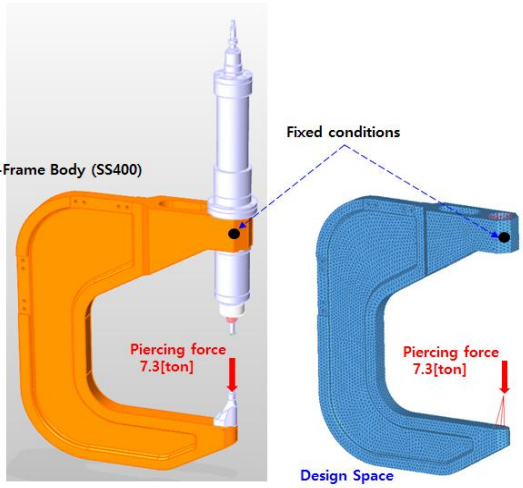

Fig. 4 Original design of C-Frame for SPR joining

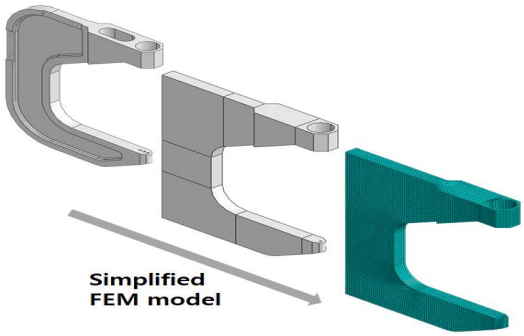

(a) Simplified model for topology optimization

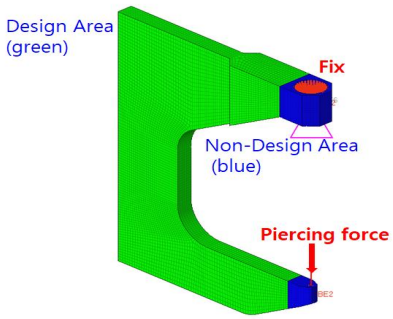

(b) Definition of Design/Non-Design Space

Fig. 5 Design space for topology optimization

2. Topology design optimization

2.1 Concept design

A lightweight design to obtain high stiffness, high strength, and reduced inertial load is the design objective with contrasting characteristics. The material quantity should be increased to increase the stiffness and strength; however, it also increases the inertial load, acting as an unfavorable condition due to vibration and fatigue.

In topology, optimization is one of the methods in which the material distribution is determined following the load path of the structure using the load and the boundary conditions. The material outside the load path is removed to obtain lightweight, high stiffness, and high strength simultaneously. Such optimization is discretized to provide design areas, which are expressed in density values. The optimized design topology can be derived by evaluating the presence or absence of each element's density based on the objective function and constraint conditions.[7] Fig. 4 illustrates the conventional model of C-frame rivet supporting the

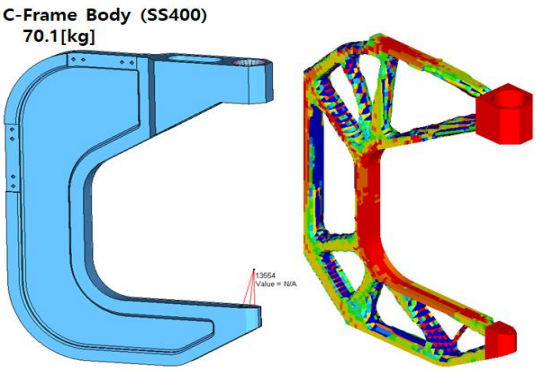

(a) Original model(left), Topology optimization model(right)

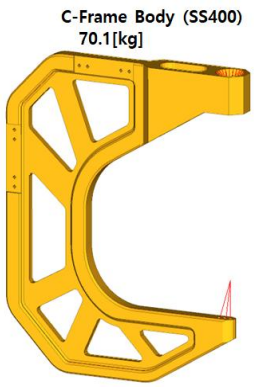

(b) Final modification model

Fig. 6 Topology optimization results

press-fit force load of 7.3 tons.

For a conventional model containing the H section (Fig. 5), the design space was defined by oversimplifying the design and a hydraulic damper with the top plate fixed as the boundary condition. Furthermore, the load transfer pathway acting on the C-frame structure was identified with the load point in which the load applies to the bottom plate mold.

The compliance minimization problem was computed for the entire design space with pseudo-density of the elements within as a design variable to keep the displacement of load point less than the allowed limit of 3.0 mm. Fig. 6 shows the result from the load transfer path, and the model concept modified based on such pathway.

Table 1 Mechanical properties of C-Frame

	Modulus [MPa]	Strength [MPa]	
		Yield	Break
SS400	210,000	245.3	480.0

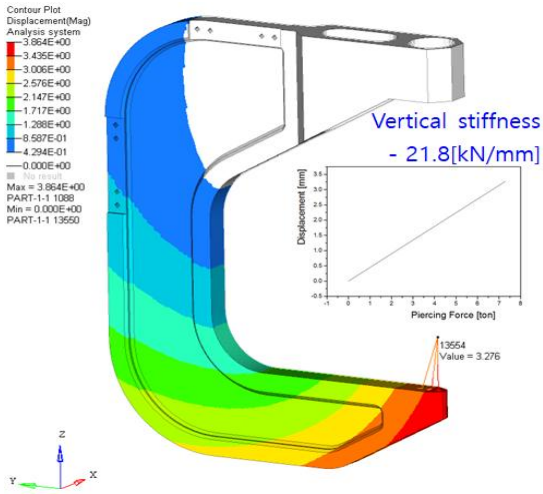

(a) Stiffness analysis result of original model

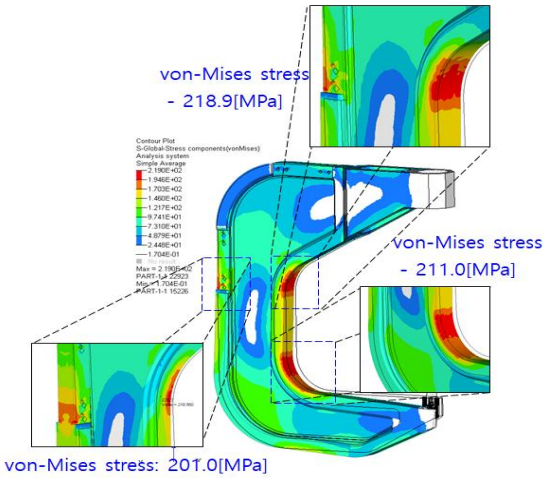

(b) Stress analysis result of original model

Fig. 7 Structural analysis results of original design

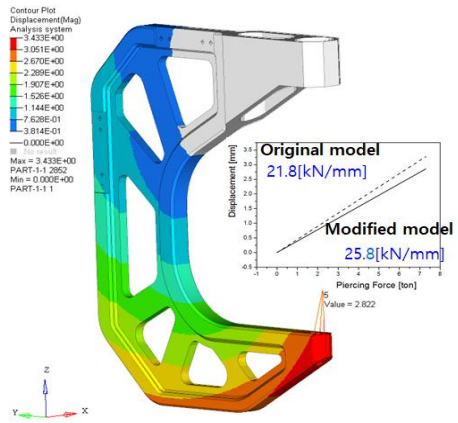

(a) Stiffness analysis result of modified model

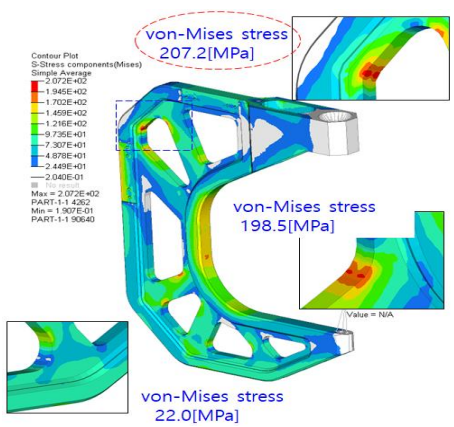

(b) Stress analysis result of modified model

Fig. 8 Structural analysis results of modified design

Table 2 Stiffness and Stress results of 2 C-Frame

	Stiffness [kN/mm]		Stress [MPa]	
Original	21.8	-	218.9	-
Modify	25.4	16.5% ↑	207.2	5.6% ↑

Table 3 Vibration modes of 2 C-Frames

	1st mode	2nd mode	3rd mode
Original	30.2	60.2	92.6
Modify	32.9	58.5	80.5

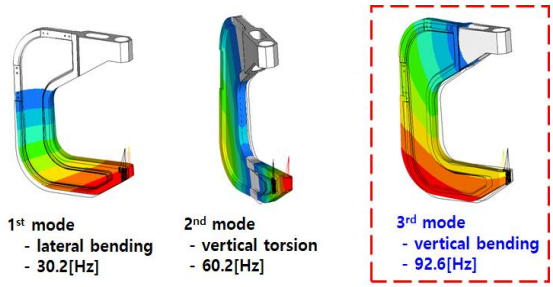

(a) original model

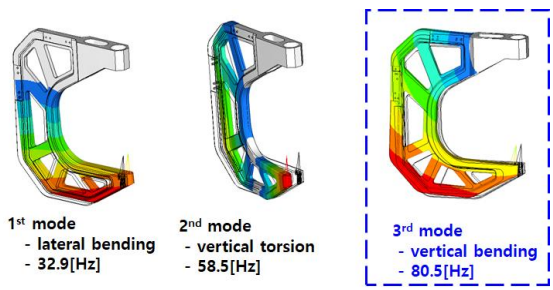

(b) modified model

Fig. 9 Vibration mode analysis results

3. Performance evaluation of design model

3.1 Review of stiffness and strength properties

The final concept model was designed (Fig. 6(b)) based on the transfer pathway of the load acting on the C-frame, as discussed in section 2.1 and Fig. 6(a). Additionally, stiffness and strength analyses were performed to compare the performance with the initial-stage design, as shown in Fig. 4. The material of the C-frame was SS400; The mechanical properties of SS400 are provided in Table 1.

The results of stiffness and strength analyses from the initial-stage model and modified concept model of the 7.3-ton rivet joined press-fit force are presented in Figs. 7 and 8, respectively. Moreover, Table 2 shows the result of the comparison of the two models for stiffness and strength. The stiffness of rivet joined press-fit force was 25.4 kN/mm, 16.6 % stronger than

that of the initially proposed design (21.8 kN/mm) because the structural reinforcement for load support was obtained by redistributing the material outside the load transfer pathway, identified through the topology optimization, to be on the pathway to reinforce the stiffness under the weight fixed to be equal. The resulting stress on the area supporting the bending load was 207.2 MPa, 5.6% higher than that of the initial model (218.9 MPa). The two models had 1.12- and 1.18-times higher safety ratios per yield stress, respectively. However, as described earlier, the stiffness of the C-frame to rivet's fit force determines the joint quality. Therefore, the final model excels in joint quality after modification with a 16.5% increase in static stiffness for an identical weight of 70.1 kg.

3.2 Review of vibration properties

The dynamic stiffness of the C-frame for dynamic load should be robust to perform the continuous procedures of rivet fastening. Thus, the natural vibration mode of the C-frame was analyzed, as shown in Fig. 9 and Table 3. Fig. 10 shows mobility response for fastening load of the rivet through a fitting.

A bending mode in the left or right lateral direction appeared as the first mode; moreover, the second mode appeared as torsional deformation of the C-frame with the vertical axis as reference. Furthermore, the third mode appeared as a vertical-axis bending mode, similar

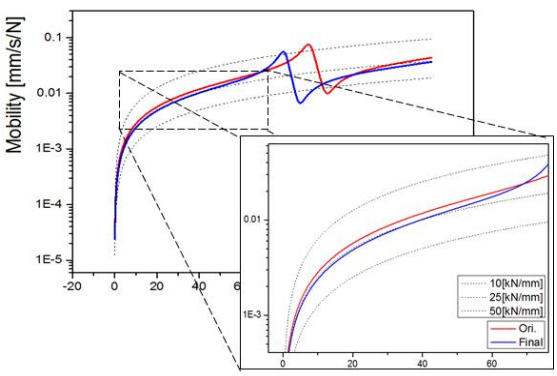

Fig. 10 Mobility response of vertical piercing load

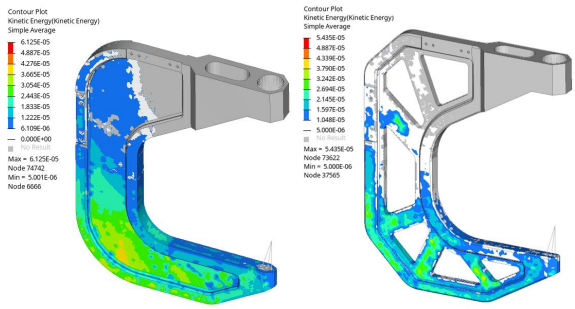

(a) Kinetic Energy of two models

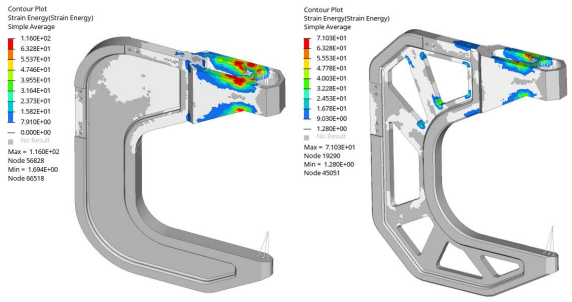

(b) Strain Energy of two models

Fig. 11 Vibration energy contour of two models

Table 4 Equivalent dynamic stiffness of 2 C-Frames

	Equi. Dyn. Stiffness [kN/mm]		Kinetic Energy	Strain Energy
Original	22.0	-	-	-
Modify	26.0	18% ↑	11.3% ↑	63.4 ↑

to the static deformation of press-fit force. The natural frequency of each mode is enlisted in Table 3. The significant deformation for the dynamic behavior of press-fit joint strength was the third vertical axis bending mode, which was 92.6 Hz and 80.5 Hz, respectively, for the initial model and the final model after modification.

Fig. 9 shows the deformation geometry of each mode. Furthermore, it illustrates mobility responses of the two models on press-fit joint load. The equivalent dynamic stiffness of the initial model and the final model after modification were 22.0 kN/mm]와 and 26.0[kN/mm], respectively. Moreover, it was 18 %

higher in the final model. The kinetic energy at the bottom part of the initial model was 11.3 % higher than the final (Fig. 11(a)). Moreover, its strain energy was also higher by 63.4%, confirming that the deformation was most likely to occur due to inertial load.

The topology optimization discussed in section 2.1 reduced the inertial load. Moreover, it could increase the dynamic stiffness of the final model after modification by 18% higher than that of the initial model through material redistribution towards the area in charge of the load. Additionally, the modified model was verified to have superior vibration characteristics even for continuous processing.

3.3 Review of fatigue properties

The fatigue properties of the C-frame were investigated for a repetitive load of rivet's fitting fastening strength using the stress states to the press-fit fastening strength in the two computed models in section 2.2 as in Fig. 6(b) and Fig. 7(b). The S-N diagram—a fatigue life graph—of the material SS400 was compared (see Fig. 12). The red and blue dotted lines represent the stress life states of the initial model and the final model after modification, respectively. A summary of the results is presented in Fig. 12 and Table 5. They show that the fatigue life of the final model after modification due to simple repetitive load showed 78.6% improvement compared to that of the initial model.

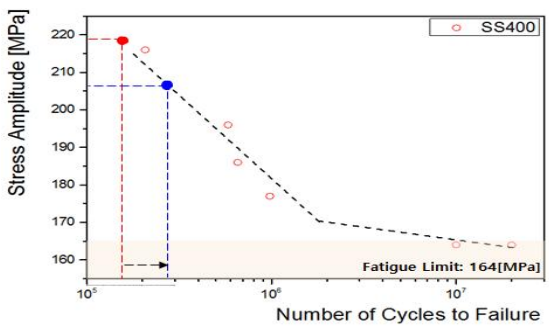

Fig. 12 Fatigue analysis results of two models

4. Stiffness test of a self-piercing rivet C-Frame

The deformation of the C-frame subject to the press-fit fastening strength was measured, as shown in Fig. 13. It was measured to verify the reliability of the results of the SPR C-frame proposed based on the results from the previous sections. The measurement was compared with the results of Fig. 7(a); these outcomes are presented in Table 5. The results from the test and analysis were 3.53 mm and 3.43 mm, respectively. Therefore, the analysis outcome was less by 0.1 mm than that of the test. Moreover, it shows higher reliability with a 2.9 % difference.

5. Conclusion

We optimized the topology design of the C-frame, supporting the load of the mold and tool, to identify the C-frame load pathway due to the press-fit force of a rivet to secure the quality of the SPR fastening. Based on this, we proposed the optimized model of stiffness and strength. We performed the analyses of fatigue, stiffness, and strength to secure the joint quality of a rivet and to test the reliability of the C-frame proposed for continuous and repetitive processing.

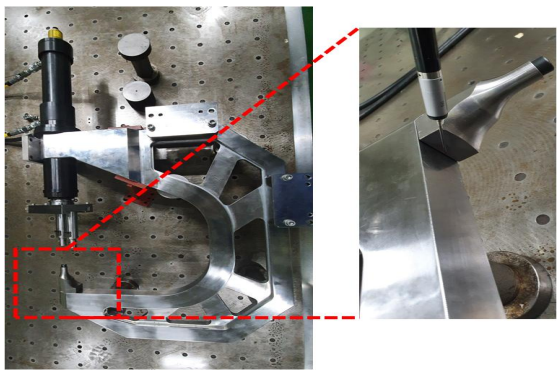

Fig. 13 Deformation measurement of a produced model

Table 5 Fatigue analysis results

	Fatigue life	
Original	1.4E+5	-
Modify	2.5E+5	78.6% ↑

Table 6 Stiffness results between TEST and CAE

	Stiffness [kN/mm]	Deformation [mm]	ratio
TEST	20.3	3.53	-
CAE	20.8	3.43	2.9% ↓

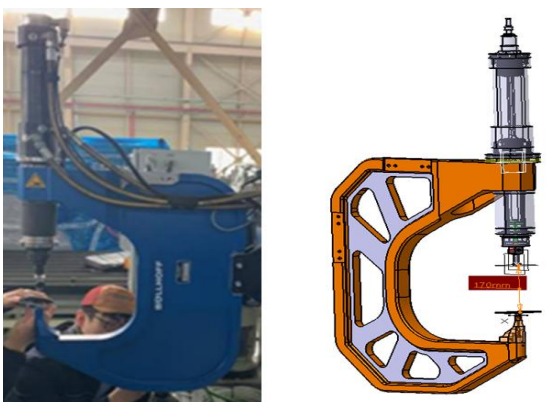

Fig. 14 Shape comparison of two models; BMT model(left), suggested model(right)

First, topology optimization was done to identify the load transfer pathway acting on the C-frame structure. The final model was proposed based on this load transfer pathway. Additionally, the analyses of stiffness and strength were done under7.3 ton press-fit force of rivet fastening to compare the design performance of the proposed concept model with that of the conventional initial model. The stiffness and strength improvement of 16.5 % and 5.6 %, respectively, can be obtained compared to the initial model.

Second, we performed a vibrational analysis. We found that the proposed final model had 18.0 % reinforcement of dynamic stiffness subject to the press-fit joint load, reviewing the reliability of continuous and repetitive procedures. The fatigue properties were improved by 78.6 % due to simplified repetitive operations. Finally, a stiffness test was conducted using fabrication of the proposed model, which showed a 2.9 % difference from the analysis result. Therefore, the proposed C-frame was verified to have superior performance than the initial model regarding SPR fastening quality and the continuous repetitive processing.

Fig. 14 shows the geometry of the C-frame proposed in this study. in comparison to the C-frame by company “B”—the BMT target model.

Acknowledgment

This study was supported by the Ministry of Trade, Industry, and Energy-Industrial Technology Innovation project, i.e., "Development of high strength aluminum 7000 series production system using thermal formation technology (Project No.: 20010987)" and by a research grant from the Korea Institute of Industrial Technology.

REFERENCES

1. Chang, I,. Cho, Y., Park, H. and So, D., Importance of Fundamental Manufacturing Technology in the Automotive Industry and the State of the Art Welding and Joining Technology, Journal of Welding and Joining, Vol. 34, No, 1, pp. 21-25, 2016.
2. Automotive Circle Int., EuroCarBody 2012, 14th Global Car Body Benchmarking Conference, (2012)
3. Website: https://www.boellhoff.com/
4. Kim, D. B., Lee, M. Y., Park, B. J., Park, J. K., Cho, H. Y., “Forging Process Design of Self-Piercing Rivet for Joining dissimilar Sheet Metals”, Journal of the Korean Society of Marine Engineering, Vol. 33, No. 6, pp. 802-807, 2012.

5. Kim, D. B., Qiu, Y. G., Cho, H. Y., “Design of self-piercing rivet to joint in advanced high strength steel and aluminium alloy sheets,” Journal of Welding and Joining, Vol. 33, No. 3, pp. 75-80, 2015
6. Kim, D. Y., Kim, D. O., Cheon, S. S., “Experimental Investigation on Fatigue Characteristics of SPR (Self-Piercing Rivet) and Hybrid Joints,” Journal of the Korean Society for Precision Engineering, Vol. 35, No. 3, pp.335-340, 2018.
7. Jung, Y. S., Lee, G. I., Kim, J. Y., “Study on Optimal Design of F-Apron of Vehicles by Multi-material Bonding,” Journal of the Korean Society of Manufacturing Process Engineers, Vol. 18, No. 2, pp. 102-107, 2019.
8. Jeong, T. E., Kim, T. E., Rhee, S. H., Kam, D. H., “Joint Quality Study of Self-piercing Riveted Aluminum and Steel Joints Depending on the Thickness and Strength of Base Metal,” Journal of Welding and Joining, Vol. 37, No. 3, pp. 212-219, 2019.